EXPERIMENTAL STUDY ON WELDING FORCES AND TEMPERATURE DURING THE DISSIMILAR FRICTION STIR WELDING OF AA7075 AND AZ31B ALLOYS

Conference Paper · October 2019

3 authors:


Musa Bilgin
Hacettepe University


Şener Karabulut
Hacettepe University


Ahmet Özdemir
Gazi University

EXPERIMENTAL STUDY ON WELDING FORCES AND TEMPERATURE DURING THE DISSIMILAR FRICTION STIR WELDING OF AA7075 AND AZ31B ALLOYS

Musa BİLGİN[a] , Şener KARABULUT[b] and Ahmet ÖZDEMİR[c]
[a] Hacettepe University, Ankara, Turkey, E-mail: musabilgin@hacettepe.edu.tr
[b] Hacettepe University, Ankara, Turkey, E-mail: senerkarabulut@hacettepe.edu.tr
[c] Gazi University, Ankara, Turkey, E-mail: ahmetoz@gazi.edu.tr

Abstract

In the present study, AA7075-T6 aluminum and AZ31B magnesium alloys were joined by the friction stir welding (FSW) method and studied the effects of the FSW parameters on the axial force, traverse force and welding temperature during the process. A fixture was designed and produced for the FSW process and AZ31B magnesium sheet were located at the advancing side during the joining process. The FSW process was conducted using four different tool speeds, four different tool offset values, two different tool angles at constant spindle speed having with square and triangle mixer tool profiles. The welding experiments were carried out based on the Taguchi mixed-orthogonal-array, L_{16} (4^2 x 2^2) and analysis of variance (ANOVA) was used to examine the test results. Mathematical models were developed to predict the axial force, traverse force and temperature by regression analysis. The axial force was decreased with the increasing mixer tool tilt angle and the welding temperature was reduced with the increasing table feed during the FSW process. The analysis results also showed that the tool profile was the most important parameter on the traverse force.

Keywords: Dissimilar friction stir welding, AA7075-T6, AZ31B, axial and feed force, welding temperature

1. Introduction

In order to develop hybrid structures combining Aluminum (Al) and Magnesium (Mg) alloys, both alloys must be reliably joined. However, due to their different metallurgical, physical and mechanical properties, the welding of dissimilar metals poses various difficulties.

The friction stir welding (FSW) method was developed by TWI (The Welding Institute) in 1991 [1] and considered as one of the most important welding methods found in the last 20 years. The FSW method is one of the most suitable methods for overcoming the disadvantages of fusion welding methods of Al/Mg alloys. The formation of intermetallic compounds is reduced due to the low heat input during the welding process and a high strength joint can be achieved by FSW method.

The important parameters for joining the same type of material by FSW method are tool design, speed, feed rate, tool tilt angle and axial plunge force [2,3], while in combination of different types of materials, the positions of different materials and tool offset are also significant welding parameters [4].

In the FSW method, simultaneous linear and rotational movement of the tool causes forces to be loaded onto the tool [5-7]. The welding parameters such as tool design, workpiece and tool material, tool rotation speed, welding speed, plunge depth, and tool angle significantly affect the forces generated during the process [8,9]. The axial force, which is the reaction force encountered by the mixing tool plunging into the materials under torque, occurs during the mixing tool plunging into the material. The axial force ensures that heat is generated by contact friction of the shoulder part of the tool to the sheets to be joined, as well as initiating the mixing process. In the FSW method, high plunging forces are required to soften the material sufficiently to ensure perfect bonding [3, 10, 11]. Keeping the forces generated during the FSW process within a certain range has a key role for perfect joint [8, 12 – 15]. Feed and axial force are critical in the improvement of process parameters in the FSW method [15 – 19].

The axial force must be sufficient for full penetration in the mixing zone. The inadequate axial force causes the deformed material to flow unsuitably the vertical direction. The high axial force causes thinning of the deformed material and as a result of this, the material exits from the shoulder part of the tool and causes burr formation [4].

Predicting, monitoring and controlling forces occurring in the FSW process have many advantages [8, 19]. Correct estimation of forces has many advantages such as improved tool design, tool life estimation, proper clamping design, clamping force estimation, and selection of suitable welding machine [20]. These advantages, which keep the forces in the appropriate range, reduce costs and increase efficiency [21].

$Al_{12}Mg_{17}$ and Al_3Mg_2 intermetallic compounds, which adversely affect the welding quality in the welding of Al and Mg alloys, are directly accured by the heat input generated during the process. Increased heat input causes an increase in intermetallic compounds. While there is a direct proportional relationship between the heat input formed during FSW and tool rotation speed, and there is an inversely proportional relationship between the spindle speed and tool travel speed [22, 23].

The temperature value formed during FSW process is higher than the Al/Mg eutectic temperature, indicating that liquefaction may occur in the mixing zone which weakens the Al-Mg interface and causes hot crack [23]. Liquid film formations can be converted to intermetallic compounds after FSW procedure and cause cold crack formation [24]. Due to the high temperatures generated during the process, the material becomes more plasticized, goes out of the mixing zone and adheres to the seam edge [25].

In this study, welding forces and temperatures were monitored during the process, the influences of the welding quality of dissimilar metals were elucidated. The experimental results were evaluated by analysis of variance (ANOVA) and prediction equations were developed for welding force and temperature by regression analysis.

2. Material Method

The AA7075-T6 aluminum and AZ31B magnesium alloys with dimensions of 300 mm × 100 mm × 5 mm used in the experiments. The mixer tool was produced K10 quality carbide in FSW process and technical view was given in Fig.1.

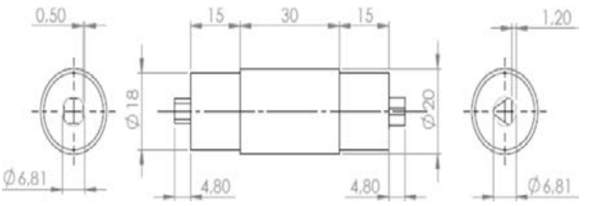

Figure 1. Triangle and square pin profile mixer tip

Welding operations were carried out on TOS OLOMOUC FGU 32 universal milling machine. In order to measure the axial force and feed force generated during the process, a special clamping apparatus is produced. Axial force and feed force was measured with S type and flat type load cells. ESIT brand PWI D model desktop indicator was preferred for instant reading and transferring of data from load cells to computer. The instantaneous recording and monitoring of the values obtained from the indicator was performed with the data logger software developed by ESIT company. Temperature measurement was made with Raytek MI3 2M digital pyrometer with ± (0.5% reading + 2 °C) accuracy

In welding processes, hot air was employed to the welded zone in order to make controlled cooling in the welded zone. Furthermore, the top plate of the apparatus is made of AA7075-T6 to ensure a uniform distribution of the heat generated during processing into the joined plates. In this way, it is aimed to prevent sudden cooling of welded samples and subsequent cracking by residual stresses. XYTRONIC brand LF 853D model hot air blowing device was mounted on test device for hot air blowing process. The test setup was presented in Fig.2.

The welding process was carried out with Taguchi L_{16} ($4^2 \times 2^2$) experimental design (Table 1). During the FSW, the AZ31B and AA7075-T6 alloy plates were located on the advancing side (AS) and the retreating side (RS), respectively. The tool was offset to AZ31B (AS).

Plunging of the mixer tool into the material was performed at 6 mm/min plunge feed, which is the lowest feed rate of the machine tool. After reached to the desired position, the temperature was controlled by pyrometer and the mixer was kept in the plunging position for one minute until the required temperature level was obtained.

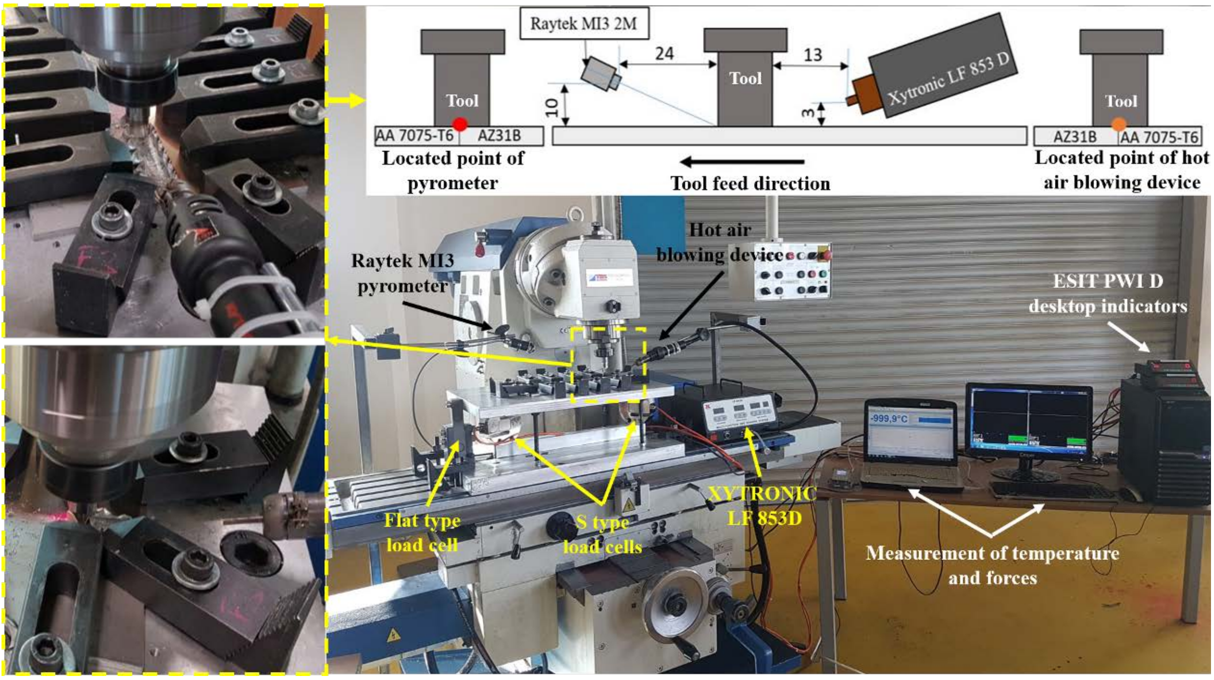

Figure 2. FSW test setup

Table 1. Process parameters used in FSW process.

Factor	Unit	Level 1	Level 2	Level 3	Level 4
Spindle speed	rev/min	500			
Travel speed	mm/min	20	25	30	36
Offset	mm	0	0,2	0.4	0.8
Tilt Angle	Degree	0°	1°		
Pin profile		Triangle	Square		

3. Discussion

The process parameters determined by Taguchi L_{16} experimental design are given in Table 2. Experimental numbers are given for systematic evaluation of the joining.

Table 2. Taguchi L16 process parameters

Exp. No	Travel speed, mm/min	Offset, mm	Tilt angle,°	Tool pin profile
M1	20	0	0	Square
M2	20	0,2	0	Square
M3	20	0.4	1	Triangle
M4	20	0.8	1	Triangle
M5	25	0	0	Triangle
M6	25	0.2	0	Triangle
M7	25	0.4	1	Square
M8	25	0.8	1	Square
M9	30	0	1	Square
M10	30	0.2	1	Square
M11	30	0.4	0	Triangle
M12	30	0.8	0	Triangle
M13	36	0	1	Triangle
M14	36	0.2	1	Triangle
M15	36	0.4	0	Square
M16	36	0.8	0	Square

The axial force, feed force and temperature values obtained in the assemblies are given in Figure 3.

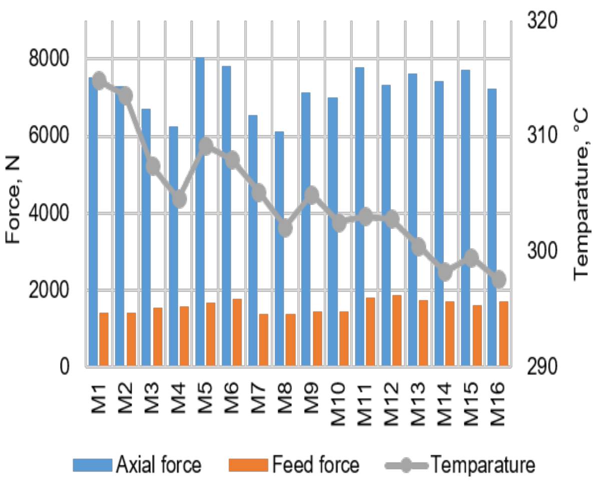

Figure 3. The temperature, axial force and feed force values measured from the tests.

The test results depicted that the temperature values were reduced when the mixing tool was located on the advancing side (AZ31B) during the process due to the lower friction value of the Mg alloy. The temperature values were increased when the mixing tool located on the aluminum side during the process. This can be attributed that the surface-centered cubic structure of the Al alloy. The presence of more active shear plane during plastic deformation, more heat is generated [14, 24, 26].

It can be also stated that there is a correlation between the axial force and temperature, whereas there is an inverse ratio between feed force and temperature. As the axial force increases, the temperature increases due to increased friction. Since the plastic deformation in the mixing zone will be more difficult with the reduction of the temperature, an increase in the feed force to which the tool is exposed is observed.

The main effect graphs (Figure 4) and ANOVA results showed (Table 3) that the most effective parameter is welding speed with 70.13%.

Table 3. Effect of independent variables on dependent variables (ANOVA)

Source	DF	Adj SS	Adj MS	F Value	P Value	Effect rate %
TEMPERATURE						
Regression	4	363.928	90.982	119.91	0	
Travel speed, mm/min	1	261.087	261.087	344.09	0	70.13
Ofset, mm	1	67.221	67.221	88.59	0	18.06
Tilt angle, °	1	32.948	32.948	43.42	0	8.85
Pin profile	1	2.673	2.673	3.52	0.087	0.72
Error	11	8.347	0.759			2.24
Total	15	372.275				100
AXIAL FORCE						
Regression	4	4867116	1216779	1027.4	0	
Travel speed, mm/min	1	688835	688835	581.63	0	14.12
Ofset, mm	1	1618739	1618739	1366.8	0	33.17
Tilt angle, °	1	2187441	2187441	1846.99	0	44.82
Pin profile	1	372100	372100	314.19	0	7.62
Error	11	13028	1184			0.27
Total	15	4880143				100
FEED FORCE						
Regression	4	397372	99343	92.5	0	
Travel speed, mm/min	1	101924	101924	94.9	0	24.91
Ofset, mm	1	7882	7882	7.34	0.02	1.92
Tilt angle, °	1	68774	68774	64.04	0	16.81
Pin profile	1	218792	218792	203.72	0	53.47
Error	11	11814	1074			2.89
Total	15	409186				100

As the welding speed increases, the tool distance increases and the temperature value decreases due to the decrease in friction time. The other two important parameters on temperature are the offset amount with 18.06% and the tool angle with 8.85%.

The decrease in the temperature by increasing of the tool angle is associated with the reduced friction area as a result of the increased tool angle and the incomplete contact of the tool shoulder to the assembly line.

The tool travel speed, tool pin profile and tilt angle exhibited the same effect on the axial and feed force. However, the axial force was decreased with increasing tool offset value and the feed force was increased with increasing tool offset value (Fig.4).

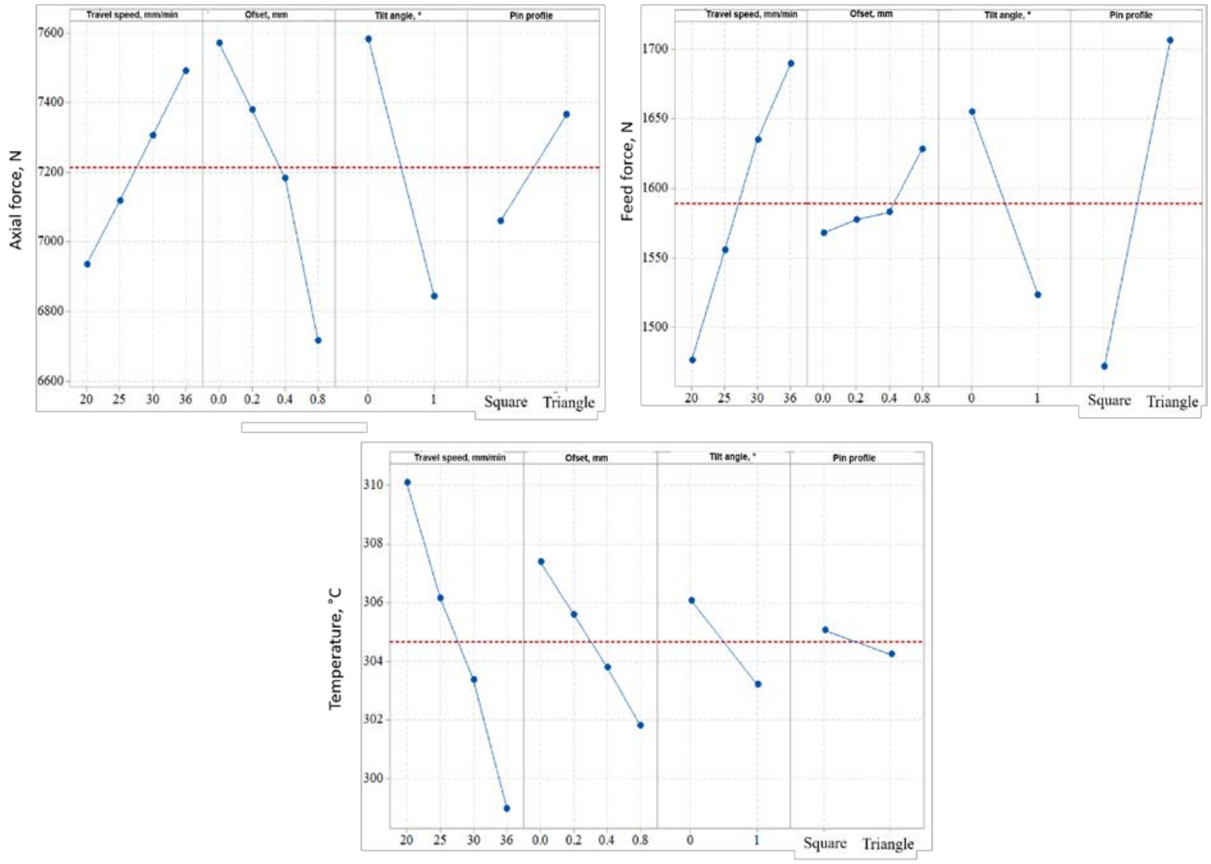

Figure 4. Effect of process parameters on average temperature in welding processes

The decreasing axial force can be explained due to the lower mechanical properties of the Mg alloy and the increasing feed force could be attributed to reducing welding temperature.

The regression analysis was performed to determine the effect rates of the welding variables on temperature, feed and axial force and the results are given in Table 3.

The most important parameter on axial force is the tool angle with an effective rate of 44.82%. The tool angle also affects the feed force in the same way. The effect of the tool angle on the feed force is 16.80% because of the reducing plunge depth depending on the increasing tilt angle.

While the tool type is the most important parameter in the feed force, its effect on the axial force is much lower. The influence rate on the feed force and axial force is 53.47% and 7.62%, respectively. By selecting the tool type as a triangle, the increased feed force is due to the fact that each edge sweeps more material per unit time due to the reduced number of edges in the pin. The slight increase in the axial force is thought to be caused by the changing material flow as well as the decreased temperature.

As the tool travel speed increases, both the axial force and the feed force increase. The effect of the feed rate on the feed force is 24.90%, while the effect on the axial force is 14.11%. The increase of the travel speed and the increase of both types of force is a result of increased heat input and increased steps of welding.

The mathematical equations are given below:

R^2 value of the equation developed for axial force estimation 99.73%.

$$EK = 6531.4 + 34.98 \times f - 1075.3 \times T_K - 739.5 \times T_A + 305 \times T_P \quad (1)$$

R^2 value of the equation developed for feed force estimation is 97.11%.

$$IK = 904.2 + 13.46 \times f + 75 \times T_K - 131.1 \times T_A + 233.9 \times T_P \quad (2)$$

R^2 value of the equation developed for average process temperature estimation is 97.76%.

$$S = 328.62 - 0.681 \times f - 6.929 \times T_K - 2.87 \times T_A - 0.817 \times T_P \quad (3)$$

Where f is feed rate, T_K is tool offset, T_A is tool tilt angle and T_P is tool pin profile (square profile: 1, triangular profile: 2) and EK is axial force, IK is feed force and S is temperature.

4. Conclusions

In this study, AZ31B magnesium and AA7075-T6 aluminum alloys were joined with the FSW method and the effects of process parameters on temperature, axial force, and feed force were investigated by ANOVA. The experimental results can be summarized as follow:

The change in the heat input directly affects the forces generated during the process.

The most effective parameters on temperature are respectively; welding speed, tool offset, tool tilt angle and pin profile.

The most effective parameters on axial force are respectively; tool tilt angle, tool offset, welding speed, and pin profile.

The most effective parameters on feed force are respectively; pin profile, welding speed, tool tilt angle and tool offset.

The atomic structure has a remarkable effect on the temperature and axial force.

Acknowledgment

We would like to thank ASO Technical College, which contributed to the study with the machine tool and the facilities, and Gazi University Scientific Research Projects Unit, which supported this project with the project numbered 59/2016-01.

5. References

[1] Thomas, W. M., Nicholas, E. D., Needham, J. C., Murch, M. G., Temple-Smith, P. and Dawes, C. J., Friction butt welding. *International Patent Application No*. PCT/GB92/02203 and GB Patent Application No. 9125978.8, Dec. 1991; *U.S. Patent Application No*. 5460317, Oct. 1995

[2] Mishra, R. S. and Ma, Z. Y., Friction stir welding and processing. *Materials Science and Engineering*, *R 50*, 1–78, 2005, doi:10.1016/j.mser.2005.07.001

[3] Rai, R., De, A., Bhadeshia, H. K. D. H. and DebRoy, T. (2011). Review: friction stir welding tools. *Science and Technology of Welding and Joining*, Vol *16*(4), p. 325–342. doi:10.1179/1362171811Y.0000000023

[4] Mehta, K. P. and Badheka, V. J., A review on dissimilar friction stir welding of copper to aluminum: Process, properties, and variants. *Materials and Manufacturing Processes*, Vol *31*(3), p. 233–254, 2016, doi:10.1080/10426914.2015.1025971

[5] Sorensen, C. D. and Stahl, A. L., Experimental measurements of load distributions on friction stir weld pin tools. *Metallurgical and Materials Transactions B: Process Metallurgy and Materials Processing Science*, Vol *38*(3), p. 451–459, 2007.

[6] Mehta, M., Arora, A., De, A. and Debroy, T., Tool geometry for friction stir welding - Optimum shoulder diameter. *Metallurgical and Materials Transactions A: Physical Metallurgy and Materials Science*, Vol *42*(9), p. 2716–2722, 2011. doi:10.1007/s11661-011-0672-5

[7] Arora, A., Mehta, M., De, A. and Debroy, T., Load bearing capacity of tool pin during friction stir welding. *International Journal of Advanced Manufacturing Technology*, Vol *61*(9–12), p. 911–920, 2012. doi:10.1007/s00170-011-3759-7

[8] Nandan, R., Roy, G. G., Debroy, T. and Introduction, I. Numerical Simulation of Three-Dimensional Heat Transfer and Plastic Flow During Friction Stir Welding. *Metallurgical and Materials Transactions A*, Vol. *37*(4), p. 1247–1259, 2006. doi:10.1007/s11661-006-1076-9

[9] Das, H., Jana, S. S., Pal, T. K. and De, A., Numerical and experimental investigation on friction stir lap welding of aluminium to steel. *Science and Technology of Welding and Joining*, Vol. *19*(1), p. 69–75, 2014. doi:10.1179/1362171813Y.0000000166

[10]Mehta, M., Chatterjee, K. and De, A., Monitoring torque and traverse force in friction stir welding from input electrical signatures of driving motors. *Science and Technology of Welding and Joining*, *18*(3), 191–197, 2013. doi:10.1179/1362171812Y.0000000084

[11]Su, H., Wu, C. S., Pittner, A. and Rethmeier, M., Simultaneous measurement of tool torque, traverse force and axial force in friction stir welding. *Journal of Manufacturing Processes*, Vol *15*(4), p. 495–500, 2013. doi:10.1016/j.jmapro.2013.09.001

[12] Bilgin, M., Karabulut, Ş. and Özdemir, A., The effect of material pairs on the axial force, traverse force and temperature in the friction stir welding process. *ICENS 2017* (p. 812–818). Budapeşte, 2017

[13] Bilgin, M., Karabulut, Ş., Özdemir, A. and Kayır, Y., The effect of the process parameters on the axial force and traverse force ın the friction stir welding of Al 7075 T6 and AZ91D. *ICENS 2017* (ss. 819–825). Budapeşte, 2017.

[14] Bilgin, M., Karabulut, Ş. and Özdemir, A. Alüminyum Magnezyum Alaşımlarının Sürtünme Karıştırma Kaynağı İle Kaynak Edilebilirliğinin Değerlendirilmesi. *Gazi Üniversitesi Fen Bilimleri Dergisi Part C: Tasarım ve Teknoloji*, Vol *5*(2), p. 191–209, 2017.

[15] Bilgin, M., Alüminyum / Magnezyum (Al / Mg) malzeme çiftinin sürtünme karıştırma kaynağı ile kaynak edilebilirliğinin araştırılması, Gazi Üniversitesi, Fen Bilimleri Enstitüsü, Doktora Tezi, 2019.

[16] Schmidt, H. B. and Hattel, J. H., Thermal modelling of friction stir welding. *Scripta Materialia*, Vol *58*(5), p. 332–337, 2008. doi:10.1016/j.scriptamat.2007.10.008

[17] Schmidt, H., Hattel, J. and Wert, J., An analytical model for the heat generation in friction stir welding. *Modelling and Simulation in Materials Science and Engineering*, Vol *12*(1), p. 143–157, 2004. doi:10.1088/0965-0393/12/1/013

[18] Khandkar, M. Z. H., Khan, J. A. and Reynolds, A. P., Prediction of temperature distribution and thermal

history during friction stir welding: input torque based model. *Science and Technology of Welding and Joining*, Vol. *8*(3), p. 165–174, 2003. doi:10.1179/136217103225010943

[19]Colligan, K. J. and Mishra, R. S., A conceptual model for the process variables related to heat generation in friction stir welding of aluminum. *Scripta Materialia*, Vol *58*(5), p. 327–331, 2008. doi:10.1016/j.scriptamat.2007.10.015

[20] Shahi, P., Barmouz, M. and Asadi, P., *Force and torque in friction stir welding*. *Advances in Friction-Stir Welding and Processing*. Woodhead Publishing Limited, 2014. doi:10.1533/9780857094551.459

[21] Trimble, D., Monaghan, J. and O'Donnell, G. E., Force generation during friction stir welding of AA2024-T3. *CIRP Annals - Manufacturing Technology*, Vol *61*(1), p. 9–12, 2012, doi:10.1016/j.cirp.2012.03.024

[22] Burak, M. and Meran, C., The effect of tool rotational and traverse speed on friction stir weldability of AISI 430 ferritic stainless steels. *Materials and Design*, Vol *33*, p. 376–383, 2012, doi:10.1016/j.matdes.2011.04.013

[23]Pourahmad, P. and Abbasi, M., Materials flow and phase transformation in friction stir welding of Al 6013/Mg. *Transactions of Nonferrous Metals Society of China (English Edition)*, vol. *23*(5), p. 1253–1261, 2013. doi:10.1016/S1003-6326(13)62590-X

[24] Azizieh, M., Alavijeh, A. S., Abbasi, M., Balak, Z. and Kim, H. S., Mechanical properties and microstructural evaluation of AA1100 to AZ31 dissimilar friction stir welds. *Materials Chemistry and Physics journal*, vol. *171*, p. 251–260, 2016. doi:10.1115/DETC2007-35287

[25] Bergmann, J. P., Schuerer, R. and Ritter, K., Friction Stir Welding of Tailored Blanks of Aluminum and Magnesium Alloys. *Key Engineering Materials*, Vol *549*, p. 492–499, 2013. doi:10.4028/www.scientific.net/KEM.549.492

[26] Zettler, B. R., Augusto, A., Rodrigues, S. and Blanco, A., Dissimilar Al to Mg alloy friction stir welds. *Advanced Engineering Materials*, vol *8*(5), p. 415–421, 2006. doi:10.1002/adem.200600030